

Comparison of Si/C/N pre-ceramics obtained by laser pyrolysis or furnace thermolysis

Anita Müller^{a,*}, Nathalie Herlin-Boime^b, François Ténégal^b, Xavier Armand^b, Frank Berger^c, Anne Marie Flank^d, Romuald Dez^b, Klaus Müller^c, Joachim Bill^a, Fritz Aldinger^a

^aMax-Planck-Institut für Metallforschung and Institut für Nichtmetallische Anorganische Materialien, Pulvermetallurgisches Laboratorium, Universität Stuttgart, Heisenbergstr. 3, 70569 Stuttgart, Germany

^bLaboratoire Francis Perrin (CEA-CNRS URA 2453), DSM-Service des Photons, Atomes et Molécules, Bât. 522, 91191 GIF-sur-Yvette Cedex, France

^cInstitut für Physikalische Chemie, Universität Stuttgart, Pfaffenwaldring 55, 70569 Stuttgart, Germany

^dLaboratoire pour l'Utilisation du Rayonnement Electromagnétique, Université Paris sud, Bat 209 D, BP34, 91898 Orsay Cedex, France

Received 20 October 2001; received in revised form 22 February 2002; accepted 3 March 2002

Abstract

This paper reports a comparison between two different methods used for the synthesis of amorphous Si/C/N pre-ceramics: the laser pyrolysis method, coupled with an aerosol generator, and thermolysis in a furnace in an inert gas atmosphere. The same precursor, liquid oligomethylvinylsilazane (OMVS, $[-(\text{CH}_3)\text{Si}(\text{HC}=\text{CH}_2)\text{NH}-]_n$) has been chosen to establish this comparison. Laser spray pyrolysis of OMVS produces nano-sized powder particles with a specific surface area of about 120 m²/g. The characteristics of the as-formed Si/C/N nanopowders (chemical composition, local order, structural evolution...) are compared to those of pre-ceramic samples obtained by thermolysis in a furnace (at 800 and 1050 °C). The amorphous network of the as-pyrolysed materials mainly consists of SiC_xN_{4-x} ($x=0,1,2$) units and amorphous or sp²-hybridized carbon. The carbon and hydrogen contents are higher in samples obtained by laser spray pyrolysis. Heat-treatment experiments at temperatures up to 1550 °C were performed to investigate the high temperature behaviour of the various samples. Decomposition was observed at about 1500 °C. © 2002 Elsevier Science Ltd. All rights reserved.

Keywords: Powders-chemical preparation; Precursors-organometallic; Si/C/N

1. Introduction

Many ceramic composites based on silicon nitride and/or silicon carbide exhibit high hardness and strength combined with creep and corrosion resistance. Therefore they are suitable materials for high temperature applications. Bulk monoliths are usually produced by sintering and densification of ceramic powders with the help of oxidic additives like Al₂O₃ and Y₂O₃.^{1–3} Another approach for the synthesis of pre-ceramic multicomposite materials is the precursor route. Silicon-containing precursors can be decomposed to produce an amorphous inorganic network. This process offers the means for the design of ceramic microstructures on an atomic scale. The properties of the produced ceramic

materials are strongly influenced by the composition and molecular structure of the precursor. A wide variety of single source precursors or precursor mixtures including silanes, silazanes and carbosilanes has been used for the synthesis of pre-ceramic materials in the Si/C/N system.⁴ Different pyrolysis techniques (chemical vapour deposition, laser pyrolysis, furnace thermolysis, microwaves etc.) were applied depending on physical characteristics of the starting materials. The ceramization behaviour of many precursors was studied intensively for each experimental set-up thus allowing for a detailed description of the chemical reactions involved. However, the comparison between the different methods is difficult because most often, different sets of precursors were used when different techniques were applied. In this study, we mainly focus on a comparison between Si/C/N pre-ceramic materials produced from liquid precursors by two different pyrolysis methods, namely furnace thermolysis and laser spray pyrolysis.

* Corresponding author. Tel.: +49-711-6861-226.

E-mail address: amueller@aldix.mpi-stuttgart.mpg.de (A. Müller).

In furnace thermolysis experiments,^{5–8} only cross-linked polymers or precursors exhibiting “latent reactivity” are applicable since monomeric or small oligomeric molecules evaporate during the long-term heat-treatment leading to a significant decrease of the ceramic yield. Therefore, mainly cross-linked polysilanes, polycarbosilanes and oligosilazanes were used.⁸

Laser pyrolysis by CO₂ laser is not very widely spread although it was initiated 20 years ago.⁹ This method is quite versatile and has been applied to produce various coatings¹⁰ and nanopowders.¹¹ Some important characteristic features of the method are the very well defined reaction zone (wall less reactor) and the very fast energy absorption of the precursor which leads to almost immediate bond cleavages followed by recombination reactions resulting in the formation of a mainly inorganic product. Monomeric precursors such as hexamethyldisilazane (HMDS)^{12–17} as well as oligomeric silazanes^{13,14} can be injected in vapour phase^{12,15} or as an aerosol^{13–17} into the laser beam to produce Si/C/N powders.

In this work, oligomethylvinylsilazane (OMVS) was used as single-source precursor for the synthesis of Si/C/N pre-ceramics because of its low viscosity (required by the aerosol generator of the laser pyrolysis set-up) and its cross-linking ability due to the presence of vinyl groups which is necessary to improve the ceramic yield during furnace thermolysis. To achieve comparison between the synthesis methods we used the same organometallic precursor in both experimental set-ups. Structural differences and common grounds of the obtained materials will be discussed in detail by means of results on elemental composition, IR, NMR spectroscopy and EXAFS/XANES.

2. Experimental

2.1. General comments

Oligomethylvinylsilazane (OMVS) was synthesized according to the procedure described in the literature^{7,18} by ammonolysis of dichloromethylvinylsilane. Furnace thermolysis experiments were performed according to Ref. 19 by heating the oligomer to 1050 °C in an argon atmosphere. The laser spray pyrolysis method has already been published.^{16,17} A brief description is given below. The products of both techniques are powders, they are referred to in the following as furnace samples and laser samples, respectively.

2.2. Experimental set-ups

2.2.1. Thermolysis in a furnace

The thermolysis of organometallic precursors can be performed by heating liquid or solid (shaped) polymers

slowly up to about 1000 °C in a flowing gas atmosphere in quartz glass Schlenk tubes. With increasing the temperature, the reaction of organic groups leads to further cross-linking of the molecules and evaporation of gaseous species and finally to the formation of an amorphous pre-ceramic network. Thermolysis of unprocessed unshaped polymers usually delivers porous grains or powders of μm to mm size. The ceramic yield depends on the chemical composition, the structure and the cross-linking of the precursor.

2.2.2. Laser spray pyrolysis

The laser pyrolysis method^{9,11} is based on the interaction between a CO₂ laser beam and a gaseous or liquid precursor. Liquids are suitable precursors in combination with an aerosol generator. Droplets of the liquid precursor are created in the aerosol generator (Pyrosol type from RBI, Meylan, France) and are carried by inert gas (argon) into the beam of a continuous wave tuneable CO₂ laser. The laser power is usually in the 300–600 W range. The resonance between one strong IR-absorption band [$10.6 \mu\text{m}$ $\nu(\text{Si-N-Si})$] of OMVS and the corresponding high energy laser wavelength leads to molecule dissociation. Due to the high pressure (atmospheric), collisions happen and lead to the formation and growth of solid particles. During the experiment, a flame is observed and its temperature is measured by an optical pyrometer. This measurement can not be considered as absolute but can give an evolution of temperature between different experiments. Due to the low residence time in the reaction zone and to the high cooling rates the particles are of nanometric size. The reaction is confined in the centre of the reactor by a flow of inert gas (argon) and happens in a wall free reactor. Therefore, the purity of the products depends mainly on the chemical purity of the precursor. The as-formed Si/C/N nanopowders are collected on a metallic filter behind the reaction zone. The laser synthesis method of liquid precursors is versatile but two restrictions can be noted. First, it is necessary to have a resonance between the laser beam and at least one of the components' absorption bands, but many molecules absorb in this infrared zone and high power tuneable CO₂ lasers are now available. Second, only liquid precursors with a low viscosity can be used due to the technical characteristics of the aerosol generator.

2.3. Annealing experiments

Annealing treatments were performed in graphite furnaces using graphite crucibles. Laser samples were first heated at 1050 °C for 4 h in an argon atmosphere (heating rate 100 °C/h) prior to annealing. Further heat-treatments were carried out in a nitrogen atmosphere at 1400 or 1550 °C with a dwell time of 3 h and a heating rate of 120 °C/h.

2.4. Characterisation methods

The characterisation methods used in this study are chemical analysis, BET (Brauner, Emmet and Teller) specific surface area measurements, Infrared (IR) spectroscopy, Nuclear Magnetic Resonance (NMR) and Extended X-ray Absorption Fine Structure (EXAFS).

Chemical element analysis was performed using a combination of different analysis equipment (ELEMENTAR Vario EL, ELTRA CS 800 C/S Determinator, LECO TC-436 N/O Determinator) and by atom emission spectrometry (ISA JOBIN YVON JY70 Plus). Specific surface area measurements were obtained by using a Micromeritics Flowsorb 2300. Infrared spectra were recorded on a FT-IR Perkin Elmer apparatus (Model 2000) using the KBr pellet method.

Solid-state NMR experiments were performed on a Bruker MSL 300 spectrometer operating at a static magnetic field of 7.05 T (^1H frequency 300.13 MHz) using a 4 mm magic angle spinning (MAS) probe. ^{29}Si and ^{13}C NMR spectra were recorded at 59.60 and 75.47 MHz, respectively, using the Cross-Polarization (CP) technique in which a spin lock field of 62.5 kHz and a contact time of 3 ms were applied. Typical recycle delays were 6 s. All spectra were acquired using the MAS technique with a sample rotation frequency of 5 kHz. ^{29}Si and ^{13}C chemical shifts were determined relative to external standard Q_8M_8 , the trimethylsilyl ester of octameric silicate, and adamantane. These values were then expressed relative to the reference compound TMS (0 ppm).

The photoabsorption measurements were carried out at the Laboratoire pour l'Utilisation du Rayonnement Electromagnétique (LURE-Orsay) on the SA32 beamline equipped with a double-crystal [InSb (111)] monochromator which allows an energy resolution of 0.7 eV. The SuperACO storage ring was operating at 800 MeV, with a typical current of 200 mA. The incident beam was monitored by measuring the total electron drain current of a polymer foil covered by about 70 nm of Ti, and located downstream the monochromator. The photoabsorption EXAFS spectra at the Si-K-edge were recorded at room temperature and collected by measuring the total electron drain current as a function of the incident photon energy, in the 1800–2500 eV energy range and with a 1 eV step. Samples were prepared by pressing the powders on Indium foil to insure good conductivity. All experimental data were recorded relatively to the crystallised-Si (c-Si) energy edge (1839 eV at the inflexion point).

Thermogravimetric analysis (TGA) was carried out in a flowing argon atmosphere (100 cm³/min) with Netzsch STA 409 (25–1400 °C, heating rate 5 °C/min) equipment in alumina crucibles. The X-ray diffraction unit used for structural investigations of the annealed samples was a Siemens D5000/Kristalloflex ($\text{Cu-K}_{\alpha 1}$ radiation), equip-

ped with a position sensitive proportional counter and a quartz primary monochromator. The furnace samples were powdered in a WC ball mill prior to analysis.

3. Results and discussion

OMVS is a colourless, air and moisture sensitive liquid consisting of six- and eight-membered silazane rings $[(\text{H}_2\text{C}=\text{CH})\text{Si}(\text{CH}_3)\text{NH}]_n$ ($n = 3, 4$).²⁰ Molecular weight and structure of OMVS are similar to those of oligomethylsilazane (OMS) which was successfully used by Gonsalves et al.^{13,14} for the production of Si(N,C) materials by laser spray pyrolysis and furnace thermolysis. The ceramization behaviour of OMVS and OMS in furnace thermolysis experiments was investigated in detail in recent studies.^{19,21} There, it could be shown that the chemical reactions during the heat treatment of OMS also occur during thermolysis of OMVS. However, the presence of vinyl groups in OMVS caused further reactions which were not possible in OMS. $\text{H}_2\text{C}=\text{CH}-$ units were polymerised at about 300 °C and contributed to the formation of sp^2 -hybridized carbon within the ceramic material, whereas sp^2 -carbon in OMS-derived ceramics was exclusively formed by thermal decomposition of methane. Due to this “complication”, a detailed comparison of OMVS-derived materials produced by laser pyrolysis or furnace thermolysis can provide more information about the differences of the two methods.

As shown in this study, laser pyrolysis was successful to transform oligomeric OMVS to Si/C/N nanopowders. The properties of the nanopowders prepared by laser spray pyrolysis can be compared to those of samples produced by furnace thermolysis at different stages/temperatures. The former materials will be denoted in the following as laser samples and the latter as furnace samples.

3.1. Production of Si/C/N powders

Thermolysis of OMVS in a furnace up to 1400 °C produces black porous ceramic grains in 26% yield. The results of thermogravimetric analysis (TGA) in an argon atmosphere are shown in Fig. 1. The onset of the first weight loss step is observed at about 180 °C corresponding to the first boiling point of OMVS. 70 wt.% of the sample evaporate between 180 and 350 °C, mainly due to distillation of the trimer ring molecules. A second weight loss of about 4% is detected between 430 and 600 °C. Up to 1400 °C, the sample weight remains constant.

Pyrolysis experiments were performed with a laser power of 330 W (sample 1), 510 W (sample 2), and 640 W (sample 3). The respective flame temperatures were 1200, 1400, and 1600 °C. Without special optimisation

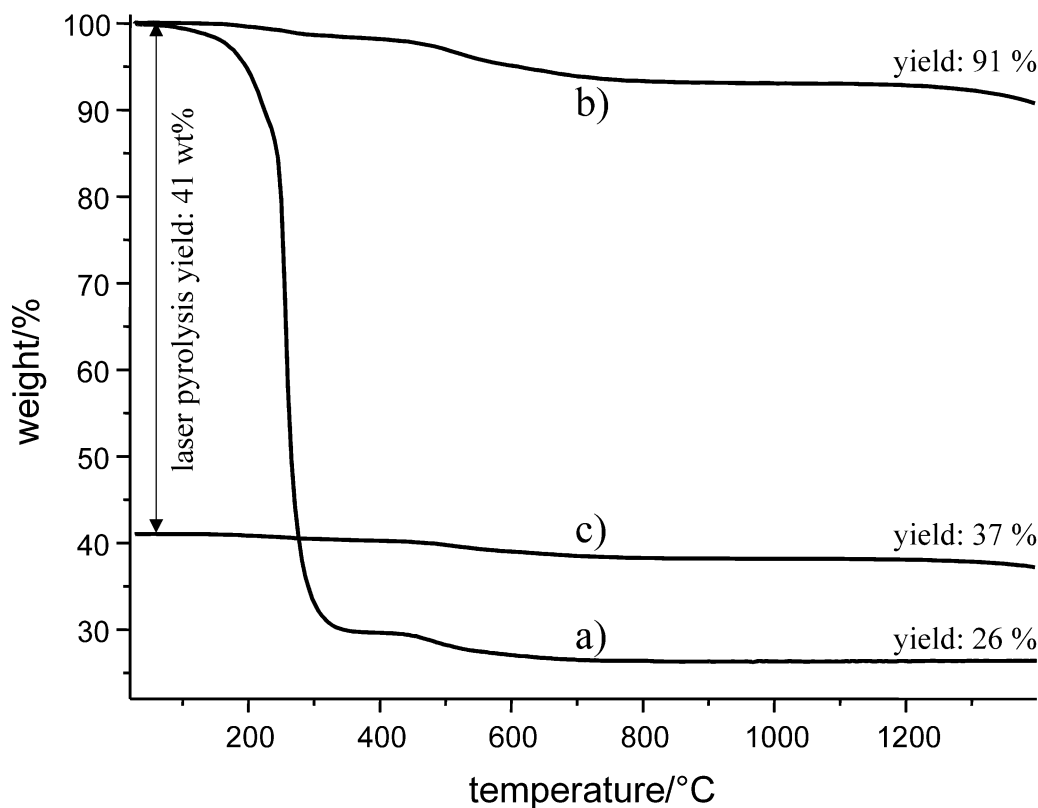


Fig. 1. TGA of (a) liquid OMVS, (b) as-formed laser sample and (c) laser sample including pyrolysis yield of 41 wt.% (20–1400 °C, heating rate 5 °C/min, Ar atmosphere).

of the experimental parameters, Si/C/N nanopowders were obtained with a production rate around 15–20 g/h for an OMVS precursor spray rate around 25–30 g/h. The conversion yield of pre-ceramic powder/used liquid OMVS was about 40 wt.%. The as-formed powders ($S_{\text{BET}} = 120\text{--}140 \text{ m}^2/\text{g}$) are dark brown to black coloured. The results of thermogravimetric analysis (TGA) of a laser sample in an argon atmosphere are shown in Fig. 1 and will be discussed below.

3.2. Comparison of as-formed laser samples and furnace samples

Table 1 shows that the three laser samples obtained with different laser power have very similar chemical compositions. Also, the IR and EXAFS spectra (not

presented here) of these samples are comparable. Obviously, variation of the laser power between 330 and 640 W has no significant effect on the chemical composition and organisation of the laser samples. Therefore in the following only one sample (sample 2) will be studied in detail.

Chemical element analysis gives an average formula $\text{SiC}_{1.7\text{--}1.8}\text{N}_{0.9}\text{H}_{0.6\text{--}0.8}\text{O}_{0.1\text{--}0.2}$ for the as-formed laser samples and $\text{SiC}_{1.6}\text{N}_{1.0}\text{H}_{0.3}\text{O}_{0.0}$ for the sample thermolysed at 1050 °C in a furnace. Both kinds of samples contain less C and H atoms than the precursor (SiC_3NH_7)_n ($n = 3, 4$). The higher O-content of the laser samples can be explained by the high surface area of these materials causing adsorption of oxygen and water. By IR or NMR spectroscopy, no evidence was found for the presence of Si–O bonds in the as-formed or annealed samples. Ignoring the O-content, the relative amount of carbon is clearly higher in the laser samples than in the furnace sample. This comparison indicates that less carbon and hydrogen and more nitrogen atoms were lost during laser pyrolysis than during furnace thermolysis.

Fig. 2 presents the IR spectra of OMVS furnace samples¹⁹ thermolysed at 800 °C (Fig. 2a) and 1050 °C (Fig. 2c) and a typical spectrum of a laser sample (Fig. 2b). All spectra show a broad absorption band between 700 and 1200 cm^{-1} , which is usually attributed

Table 1
Chemical composition of laser samples as a function of laser power and of a furnace sample after thermolysis at 1050 °C (wt.%)

Experiment	Laser power/W	Si	C	N	H	O	Formula
Laser (1)	330	44.0	32.0	20.5	0.9	3.3	$\text{SiC}_{1.7}\text{N}_{0.9}\text{H}_{0.6}\text{O}_{0.1}$
Laser (2)	510	44.0	31.1	19.6	1.2	4.4	$\text{SiC}_{1.7}\text{N}_{0.9}\text{H}_{0.8}\text{O}_{0.2}$
Laser (3)	640	43.2	34.0	19.3	1.3	3.1	$\text{SiC}_{1.8}\text{N}_{0.9}\text{H}_{0.8}\text{O}_{0.1}$
Furnace	–	45.4	31.4	22.3	0.5	0.7	$\text{SiC}_{1.6}\text{N}_{1.0}\text{H}_{0.3}\text{O}_{0.0}$

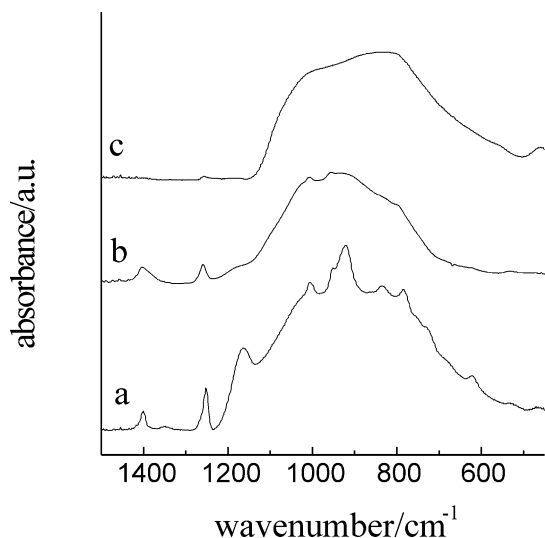


Fig. 2. Infrared spectra of (a) OMVS thermolysed at 800 °C, (b) as-formed laser powder and (c) OMVS thermolysed at 1050 °C.

to Si/C/N amorphous structures.^{14,20} In laser powders, maximum absorption was observed at 950 cm^{-1} . Therefore, Si atoms seem to be bonded mainly to N atoms [940 cm^{-1} $\nu(\text{Si-N-Si})$]. During furnace thermolysis, the absorption maximum was shifted from 920 cm^{-1} in the 800 °C sample to 835 cm^{-1} in the 1050 °C sample. The latter appears to contain more Si-C bonding [830 cm^{-1} $\nu(\text{Si-C})$]. In each spectrum, an absorption at 1260 cm^{-1} is observed. It is attributed to a Si-CH₃ deformation vibration.²² The presence of this Si-CH₃ unit indicates the incomplete pyrolysis of the precursor.^{19,20} The intensity of this band, however, is significantly decreased in the spectrum of the 1050 °C furnace sample compared to the 800 °C furnace sample while it appears in an intermediate intensity in the laser sample spectrum. Furthermore, individual absorptions could be detected in the 800 °C furnace sample spectrum whereas absorptions after thermolysis at 1050 °C were found to be very broad and featureless. Here again, the laser sample spectrum seems to represent an intermediate stage. We therefore conclude from IR analysis that the structural properties of the laser sample approximately correspond to those of a furnace sample thermolysed at about 900 °C.

The X-ray powder diffraction patterns of as-formed laser powders and furnace samples (1050 °C) do not show any diffraction peaks, demonstrating that both materials exhibit an amorphous structure. This has already been observed for different laser samples obtained from an aerosol.^{13,14,16,17,23,24} Complementary structural comparison is achieved through EXAFS and NMR.

EXAFS and XANES spectra of laser sample 2 are shown in Figs. 3 and 4, respectively. A model of the short-range order of thermolysed Si/C/N furnace samples based on diffraction data was already pub-

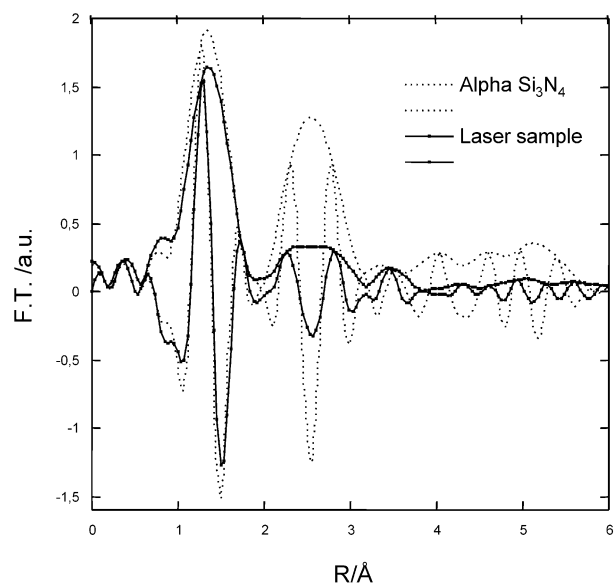


Fig. 3. Comparison of the Fourier transform (modulus and imaginary part) of the k^2 weighted EXAFS oscillations for the laser sample and for the reference alpha Si_3N_4 .

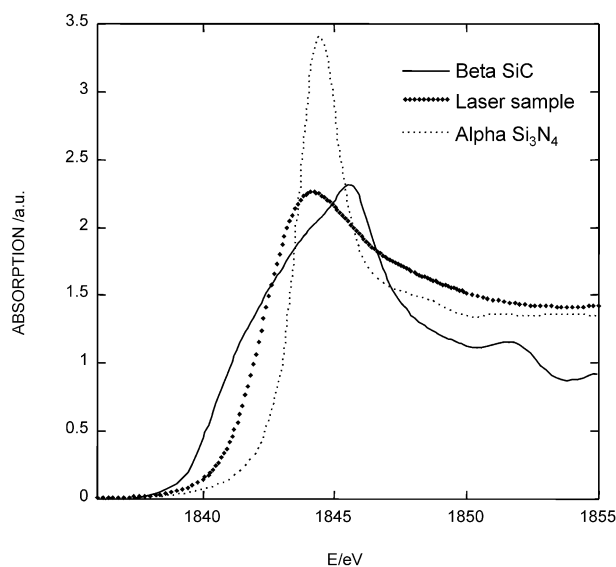


Fig. 4. Comparison of Si K edge XANES spectra of beta SiC, alpha Si_3N_4 and the laser sample.

lished.^{19,25} Therefore, characterization of these samples by EXAFS/XANES was not necessary. The EXAFS data analysis was performed on the laser sample in the following way: the oscillatory part was extracted using a 5th order polynomial fit and normalized using an Heitler approximation. Fourier Transformation (FT) of the k^2 weighted EXAFS signal was then performed over the same energy range ($2.5\text{--}10.7 \text{ \AA}^{-1}$) for all the compounds studied here. This yields a pseudo radial distribution function in R space (uncorrected from the phase shift) of the coordination shells surrounding the absorbing Si atoms, as shown in Fig. 3 for a laser sample and

α -Si₃N₄. The first and second peaks correspond to the first and second coordination shells around Si atoms. A qualitative comparison suggests an environment for the Si atoms that mainly consists of N atoms as first neighbours (an analogous comparison with β -SiC excludes an environment dominated by Si–C pairs). Furthermore, the peak corresponding to the first coordination shell was back-transformed in the *k* space and fitted using the electronic parameters extracted from the model compound α -Si₃N₄ (4 N atoms at an average distance of 1.74 Å). The best simulation was obtained with an average environment of 3.9 ± 0.3 N atoms at a distance of 1.74 ± 0.2 Å. The Debye–Waller factor was estimated to be 0.048 \AA^{-2} . A two-shell fit on the basis of Si–N and Si–C pairs for the same experimental data set only gave 0.2 ± 0.1 carbon atoms in the average environment of the silicon atoms.

Nevertheless, looking at the edge position on the XANES spectra (Fig. 4), one can not exclude the presence of mixed environments (SiC_{*x*}N_{4–*x*}) around the silicon atoms.²⁶ Furthermore, the fact that the threshold is not well defined, but spread over more than 3 eV suggests the existence of various environments. The presence of Si–C bonds is also indicated by IR (for example Si–CH₃, see Fig. 2) and NMR (see below). The fact that these Si–C bonds were not detected in the EXAFS experiments may be due to a high degree of disorder with various X–Si–C bond lengths and angles in the laser powders.

Fig. 5 presents the ¹³C and ²⁹Si MAS NMR spectra of OMVS furnace samples¹⁹ thermolysed at 800 and 1050 °C and the spectra recorded for the as-formed laser sample. In general, the peak positions are rather similar in both cases, although the NMR spectra of the various samples exhibit some characteristic differences. Thus, in the ¹³C NMR spectrum of the laser sample, the signal to noise ratio is better than for the furnace samples, while it is somewhat lower in the ²⁹Si NMR spectra of the laser sample as compared to the furnace samples. This might be due to the presence of hydrogen atoms and the cross-polarization technique used for ¹³C and ²⁹Si NMR signal detection. It is known from chemical analysis and from the IR spectra that the laser powder contains a large amount of hydrogen. The high signal to noise ratio in the ¹³C NMR spectrum and the low ratio in the ²⁹Si NMR spectrum seem to indicate that hydrogen atoms in laser samples are preferentially bonded to carbon and not to silicon atoms whereas IR spectra of furnace samples revealed the formation of Si–H bonds during thermolysis.¹⁹

The ¹³C NMR spectrum of the laser sample shows two signals at around 0 and 140 ppm with similar intensities. The signal at 0 ppm can be attributed in particular to CH_3Si groups, which is in agreement with the signature of Si–CH₃ observed in the infrared spectra. The signal at 140 ppm can be assigned to sp²-

hybridized carbon.^{27,20,19} The ¹H NMR spectra (not shown here) confirm the presence of H atoms bonded to sp²- and sp³-hybridized carbon. In addition, the furnace sample at 1050 °C exhibits a broad spectral component, centred at about 24 ppm, which can be attributed to the presence of CSi_4 units and which is completely missing for the laser sample.

In comparison to the furnace samples, the ¹³C NMR signals of the laser sample are much sharper. The broad NMR signals of the furnace samples are attributed to the amorphous character of the material and in particular to the large chemical and structural heterogeneity of the sample.¹⁹ The narrowing of the ¹³C NMR signals therefore suggests that the laser powder is less heterogeneous, i.e. all the carbon atoms possess a similar molecular surrounding.

Furthermore, the comparison of the ¹³C NMR spectra of laser and furnace samples indicates that the intensity ratio C(sp²)/C(SiCN) is higher for the laser sample. Therefore, the relative amount of “free carbon” should be higher in these materials.

The ²⁹Si NMR spectrum of the laser powder shows resonances between about 0 and –60 ppm. In contrast to the furnace samples, here again relatively sharp signals at –8, –24 and –35 ppm are observed along with a broad resonance centred at about –50 ppm. These signals can be attributed to the presence of primarily mixed tetrahedra $\text{SiC}_x\text{N}_{4-x}$ (*x* = 0, 1, 2). The presence of SiC₄ cannot completely be excluded from these data, since its resonance falls into the same spectral range.²⁰ As before, the NMR linewidth is found to be smaller than for the furnace samples which again implies a larger homogeneity of the laser sample. In addition, it might well be that unreacted groups give rise to these relatively sharp NMR signals.

From the different results presented here, it seems that the as-formed laser powder is composed of a mixture of SiC_{*x*}N_{4–*x*} (*x* = 0, 1, 2) units and free carbon with H bonded mainly to carbon atoms. The X–Si–N bond lengths and angles appear to be locally well-ordered (similar to crystalline Si₃N₄) whereas X–Si–C bond parameters vary significantly. This organisation is thus similar to the local environment of Si atoms found in furnace samples at 800 and 1050 °C. As was already observed for different Si/C/N precursor ceramics, organisation of the amorphous furnace samples starts via formation of silicon nitride structures prior to silicon carbide crystallisation.^{19,25} On the basis of the chemical analysis and the ¹³C NMR data, the amount of “free carbon” should be higher in laser samples.

3.3. Annealing treatments

The differences in local order between laser and furnace samples may induce a different behaviour during thermal treatments. Therefore, the as-formed laser

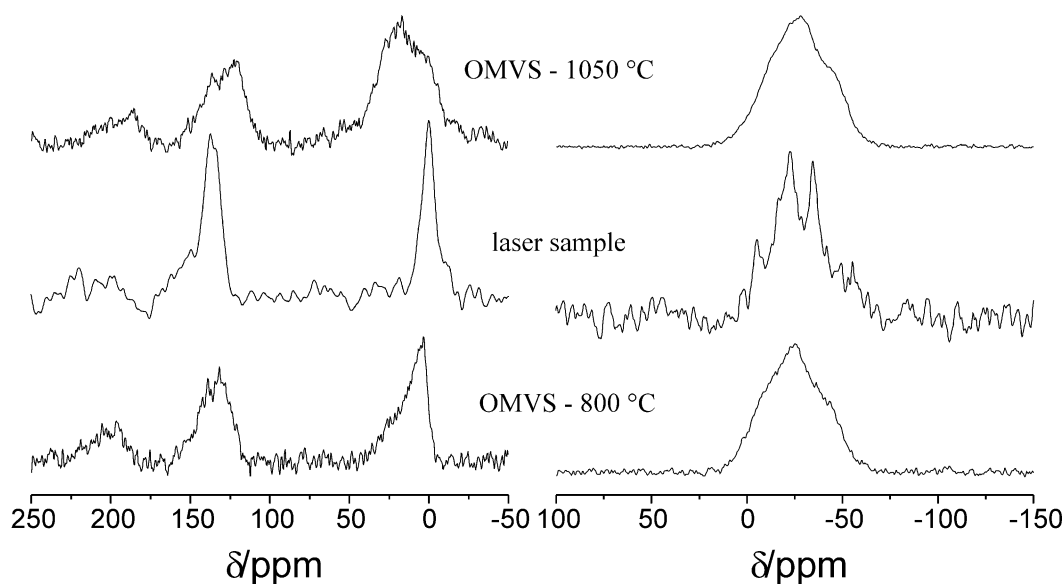


Fig. 5. ^{13}C (left column) and ^{29}Si MAS NMR (right column) spectra of OMVS after thermolysis at 800 and 1050 °C and of the as-formed laser sample. The ^{13}C NMR signals at about 200 ppm reflect spinning side bands due to sample rotation.

samples were analysed by TGA in a flowing argon atmosphere up to a temperature of 1400 °C (5 °C/min). Again, the results for the different laser samples (1, 2, and 3) are very similar, therefore, only the evolution of sample 2 is presented here. The TGA curve of as-formed laser sample 2 synthesised at 510 W is inserted in Fig. 1. Up to 1400 °C, a continuous mass loss was detected leading to a final mass reduction of about 9% at 1400 °C. Due to the large BET surface areas of the laser samples (about 120 m²/g), the materials contain adsorbed water which is mainly responsible for the weight loss detected at low temperatures. Furthermore, the mineralisation process proceeds during the heat-treatment leading to the cleavage of organic groups (CH containing units). During laser pyrolysis, liquid OMVS was transformed into preceramic laser sample 2 with a yield of 41 wt.%. The as-formed powder showing a loss of 9 wt.% of the powder mass used for TGA experiments up to 1400 °C, the overall ceramic yield at 1400 °C amounts to 37% relative to the amount of OMVS used (Fig. 1c). This value is significantly higher than that for the furnace sample (26%).

In order to investigate crystallisation and decomposition, annealing experiments were performed. Because of the different synthesis conditions of the powders (reaction time, temperature), the as-formed laser samples were first heated up to 1050 °C for 4 h in an argon atmosphere which corresponds to the thermolysis conditions of the furnace samples. Subsequent annealing was carried out with a heating rate of 2 °C/min in a nitrogen atmosphere at 1400 or 1550 °C for 3 h, respectively. At each step of the treatment, the weight loss was measured (see Table 2), and the samples were analysed by IR spectroscopy (Fig. 6) and X-ray diffraction (XRD) (Fig. 7).

At 1050 °C, a mass loss of 5% was detected for the laser sample (Table 2). The IR spectra of both laser and furnace samples (Fig. 6a) show a broad absorption band between 600 and 1200 cm⁻¹ characteristic for a superposition of Si–C and Si–N vibration bands.¹⁴ The maximum of this absorption is located at higher energies in the laser sample spectrum indicating a nitrogen-rich first co-ordination sphere of silicon atoms. In contrast to this, the furnace sample spectrum shows a distinct tailing towards lower energies characteristic for a carbon-rich environment of silicon atoms. These observations confirm the results discussed in the first part of this paper. Whereas the furnace sample spectrum appears to be without distinct structure, the laser sample still contains structural units of the precursor thermolysed at 400 °C;¹⁹ at least three corresponding absorption maxima (1050, 960, and 880 cm⁻¹) were detected. Compared to the spectrum of the as-formed laser powder, the absorption of the Si–CH₃ group at 1260 cm⁻¹ has disappeared while the shape of the broad band between 600 and 1200 cm⁻¹ remains the same after heat-treatment at 1050 °C. XRD experiments revealed that both laser and furnace samples are still amorphous at this temperature (Fig. 7).

At 1400 °C, the weight loss of the furnace sample is negligible (<1%) whereas the weight change of the 1050 °C laser sample amounts to –13% (Table 2). Compared to the TGA results (9% mass loss at 1400 °C for the laser sample), the slightly enhanced mass change can be explained by the dwell time of 3 h in the annealing experiment.

At 1400 °C, thermodynamically unstable (organic) groups are cleaved whereas the reaction of Si–N groups with C is expected at higher temperatures (1484 °C).²⁸ The observed mass change can therefore be attributed

Table 2
Weight change during annealing (annealing temperature, atmosphere, dwell time and heating rate)

	1050 °C Ar (4 h) (100 °C/h)	Laser sample 1050 °C Furnace sample	1400 °C N ₂ (3 h) (120 °C/h)	1550 °C N ₂ (3 h) (120 °C/h)
Laser sample 2	–5%		–13%	–32%
Furnace sample	0%		–0.5%	–19.5%

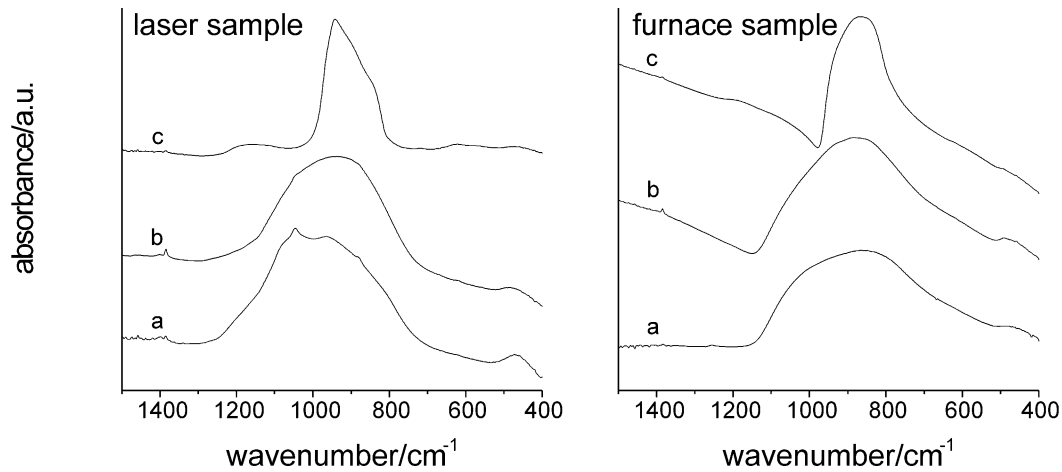


Fig. 6. IR spectra of laser samples (left column) and furnace samples (right column) heated to (a) 1050 °C and subsequently annealed at (b) 1400 or (c) 1550 °C.

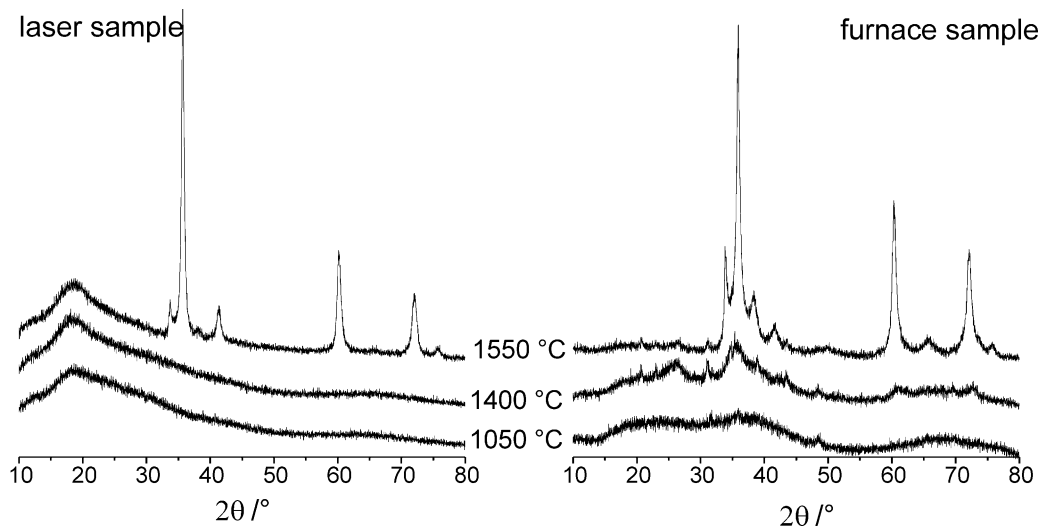


Fig. 7. XRD diagrams of laser samples (left column) and furnace samples (right) tempered at 1050 °C and subsequently annealed at 1400 or 1550 °C.

to the loss of hydrogen, hydrocarbons and adsorbed water on the surface of the particles. The SiC_xN_y vibration bands in the IR spectrum (Fig. 6b) are still very broad. In the spectra of the 1050 and 1400 °C furnace samples, their appearance is very similar showing that no significant evolution of the silicon coordination spheres occurred. The distinct structure of absorption bands in the 1050 °C laser sample spectrum, however, is absent in the 1400 °C laser sample spectrum. The energy range of the SiC_xN_y absorption band of laser samples is

slightly smaller at 1400 °C than at 1050 °C. The XRD diagram of the 1400 °C laser sample reveals an amorphous structure (Fig. 7). In the diagram of the furnace sample (Fig. 7), very broad reflection signals attributed to silicon carbide were detected. (Besides, the furnace sample contains traces of WC due to the preparation technique.) With regard to XRD, the main difference at this temperature between laser and furnace samples seems to be a lower organisation degree in the laser samples.

When heated up to 1550 °C, advanced decomposition of the materials was observed. The weight losses of 1050 °C laser and furnace samples were 32 and 20%, respectively (Table 2). According to thermodynamic calculations, Si–N bonds are not stable in the presence of carbon above 1484 °C (1 atm N₂).²⁸ Hence, evaporation of gaseous nitrogen accompanied by the formation of Si–C bonds is expected at 1550 °C. This reaction explains the weight loss observed in the furnace sample: the 20% weight loss approximately corresponds to the amount of nitrogen present in the as-formed material (22.3 wt.%, Table 1). In the as-formed laser sample, the nitrogen content is 19.6 wt.%. On the assumption that no nitrogen is lost during the heat-treatment at 1050 °C, the nitrogen content amounts to about 21.3 wt.% in the 1050 °C sample. Therefore, the enhanced mass loss of the 1050 °C laser sample (32%) at 1550 °C can not only be explained by the loss of nitrogen. At 1400 °C, the weight change of the laser sample attributed to the evaporation of H₂, hydrocarbons and adsorbed water was determined to be –13% (Table 2). This mass loss should also occur during annealing up to 1550 °C. The total weight loss of the laser sample (32%) could then correspond to evaporation of hydrogen, hydrocarbons and adsorbed water in a first step and subsequent loss of nitrogen during formation of SiC.

Both IR spectra (Fig. 6) and XRD diagrams (Fig. 7) indicate the presence of crystalline SiC. The IR spectra of furnace and laser samples after annealing at 1550 °C have a maximum at similar positions ($\approx 900\text{ cm}^{-1}$), indicating the absence of Si–N bonds and the predominance of SiC structural units. The absorption band is significantly sharper than in the spectra of 1400 °C samples. More precise information on the crystallisation is obtained from XRD diagrams. In both cases β -SiC seems to be the major phase beside a minor phase composed of α -SiC.

4. Summary and conclusion

In this study, a liquid oligomer, oligomethylvinylsilazane, previously used in furnace thermolysis experiments was transformed into Si/C/N nanopowders by laser spray pyrolysis. The structure of pre-ceramic powders produced by laser spray pyrolysis on the one hand and furnace thermolysis on the other hand was compared in detail by different techniques sensitive to the long range or short range order. The thermal behaviour during annealing was also studied.

As a first result, it was shown by IR and NMR spectroscopy that structural features of as-formed laser samples approximately correspond to those of samples obtained by furnace thermolysis of OMVS at 800/1050 °C. The chemical composition of as-formed laser nanopowders can be compared with that of furnace samples

obtained from OMVS at 1050 °C. However, the relative amount of carbon is slightly higher in laser samples whereas the nitrogen content is reduced as compared to that of furnace samples. According to EXAFS and XANES spectra of laser samples, the silicon atoms are located in the centre of mixed tetrahedra SiC_xN_{4-x} ($x=0,1,2$) with locally well ordered Si–N bonds and C atoms at varying positions. The N-rich environment around silicon atoms together with the high amount of carbon could indicate a higher content of “free carbon” in the laser sample than in the furnace sample. Even though the laser frequency was tuned on the Si–N vibration energy, the Si/N atomic ratio of the precursor remained almost constant during laser pyrolysis experiments. The laser activation of molecules seems to induce the cleavage of Si–C and N–H bonds releasing hydrocarbon radicals. Those radicals are partly lost in the gas phase but they also contribute to the formation of sp²-hybridized carbon (“free carbon”) found in the powders. This mechanism implies, that the CH_x groups of the precursor partly remain intact during laser pyrolysis. Therefore, although the energy transfer methods in laser pyrolysis and furnace thermolysis are very different, decomposition reactions of molecular precursors are comparable in both experimental set-ups.

The yield of laser pyrolysis (solid pre-ceramic material/liquid OMVS) after annealing at 1400 °C was 37 wt.%. Beginning of the SiC crystallisation of furnace samples was observed after heat-treatment at 1400 °C in a nitrogen atmosphere whereas laser samples remained X-ray amorphous at this temperature. Both laser and furnace samples exhibiting a large carbon excess, the reaction of Si–N units with “free carbon” lead to formation of SiC and nitrogen gas at higher temperatures. The mass loss detected between 1400 and 1550 °C corresponds to the amount of nitrogen present in as-formed materials.

In summary, pre-ceramic powders produced by laser spray pyrolysis or furnace thermolysis of OMVS have a great deal in common with regard to their structural organisation. The method used to decompose the precursor mainly determines the macroscopic appearance of the materials (nano-sized powders or bulk particles).

Acknowledgements

This work was supported by PROCOPE, a bilateral co-operation between France and Germany. The authors gratefully acknowledge the help of G. Kaiser (microanalytic investigations) and S. Nast (TGA).

References

1. Lange, F. F., Effect of microstructure on strength of Si₃N₄–SiC composite system. *J. Am. Ceram. Soc.*, 1973, **56**, 445–450.

2. Greil, P., Petzow, G. and Tanaka, H., Sintering and HIPping of silicon nitride carbide composite materials. *Ceram. Int.*, 1987, **13**, 19–25.
3. Lange, F. F., High-temperature strength behavior of hot-pressed Si_3N_4 : evidence for subcritical crack growth. *J. Am. Ceram. Soc.*, 1974, **57**, 84–87.
4. For an overview see: Laine, R. M. and Sellinger, A., Si-containing ceramic precursors. In *The Chemistry of Organic Silicon Compounds* Vol. 2, chapter 39, ed. Z. Rappoport and Y. Apeloig. John Wiley & Sons Ltd., 1996, 2245–2315; Bill, J. and Aldinger, F., Progress in materials synthesis. *Z. Metallkd.*, 1996, **87**, 827–840; Peuckert, M., Vaahs, T. and Brück, M., Ceramics from organometallic polymers. *Adv. Mater.*, 1990, **2**, 398–404.
5. Walker, B. E., Rice, R. W., Becher, P. F., Bender, B. A. and Coblenz, W. S., Preparation and properties of monolithic and composite ceramics produced by polymer pyrolysis. *Am. Ceram. Soc. Bull.*, 1983, **62**, 916–923.
6. Seyferth, D. and Wiseman, G. H., High-yield synthesis of $\text{Si}_3\text{N}_4/\text{SiC}$ ceramic materials by pyrolysis of a novel polyorganosilazane. *J. Am. Ceram. Soc.*, 1984, **67**, C132–C133.
7. Peuckert, M., Vaahs, T. and Brück, M., Ceramics from organometallic polymers. *Adv. Mater.*, 1990, **2**, 398–404.
8. Bill, J. and Aldinger, F., Precursor-derived covalent ceramics. *Adv. Mater.*, 1995, **7**, 775–787.
9. Cannon, W. R., Danforth, S. C., Flint, J. H., Haggerty, J. S. and Marra, R. A., Sinterable ceramic powders from laser-driven reactions. I. Process description and modeling. *J. Am. Ceram. Soc.*, 1982, **65**, 324–330.
10. See for example: Colombo, P., Martucci, A., Fogoto, O. and Villoresi, P., Silicon carbide films by laser pyrolysis of polycarbosilane. *J. Am. Ceram. Soc.*, 2001, **84**, 224–226.
11. Knudsen A. K., In *Carbide, Nitride and Boride Materials Synthesis and Processing*, ed.: A. W. Weimer, Chapman and Hall, London, 1997, pp. 343–358 and references therein.
12. Rice, R. W., Laser synthesis of Si/C/N powders from 1,1,1,3,3,3-hexamethyldisilazane. *J. Am. Ceram. Soc.*, 1986, **69**, C183–C185.
13. Magee, A. P., Strutt, P. R. and Gonsalves, K. E., Laser-induced conversion of molecular precursors to thin films and deposited layers. *Chem. Mater.*, 1990, **2**, 232–235.
14. Gonsalves, K. E., Strutt, P. R., Xiao, T. D. and Klemens, P. G., Synthesis of Si(C,N) nanoparticles by rapid laser polycondensation/crosslinking reactions of an organosilazane precursor. *J. Mater. Sci.*, 1992, **27**, 3231–3238.
15. Li, Y., Liang, Y., Zheng, F. and Hu, Z., Laser synthesis of ultrafine Si_3N_4 -SiC powders from hexamethyldisilazane. *Mater. Sci. Eng.*, 1994, **A174**, L23–L26.
16. Cauchetier, M., Croix, O., Herlin, N. and Luce, M., Nanocomposite Si/C/N powder by laser-aerosol interaction. *J. Am. Ceram. Soc.*, 1994, **77**, 993–998.
17. Herlin, N., Luce, M., Musset, E. and Cauchetier, M., Synthesis and characterization of nanocomposite Si/C/N powders by laser spray pyrolysis of hexamethyldisilazane. *J. Eur. Ceram. Soc.*, 1994, **13**, 285–291.
18. Huggins, J., *Organische Silazanpolymere, Verfahren zu ihrer Herstellung sowie ein Verfahren zur Herstellung von Keramikmaterialien daraus*. Ger. Offen. DE 411 42 17 A1, 1992.
19. Bill, J., Schuhmacher, J., Müller, K., Schempp, S., Seitz, J., Dürr, J., Lamparter, H.-P., Golczewski, J., Peng, J., Seifert, H.-J. and Aldinger, F., Investigations into the structural evolution of amorphous Si–C–N ceramics from precursors. *Z. Metallkd.*, 2000, **91**, 335–351.
20. Schuhmacher, J., *Solid State NMR Investigations of the Transformation of Polysilazanes and Polysilylcarbodiimides to Si-(B-)C–N Ceramics*. PhD thesis, Universität Stuttgart 2000, Stuttgart, Germany (in German).
21. TraBl, S., Suttor, D., Motz, G., Rössler, E. and Ziegler, G., Structural characterisation of silicon carbonitride ceramics derived from polymeric precursors. *J. Eur. Ceram. Soc.*, 2000, **20**, 215–225.
22. Lin-Vien, D., Colthup, N. B., Fateley, W. G. and Grasselli, J. G., *Handbook of Infrared and Raman Characteristic Frequencies of Organic Molecules*. Academic Press, 1991.
23. El Kortobi, Y., d’Espinoze de la Caillerie, J. B., Legrand, A. P., Armand, X., Herlin, N. and Cauchetier, M., Local composition of Oxycarbides obtained by laser spray pyrolysis. *Chem. Mater.*, 1997, **9**, 632–639.
24. Herlin, N., Armand, X., Musset, E., Martinengo, H., Luce, M. and Cauchetier, M., Nanometric Si-based oxide powders: synthesis by laser spray pyrolysis and characterization. *J. Eur. Ceram. Soc.*, 1996, **16**, 1063–1073.
25. Dürr, J., Schempp, S., Lamparter, H. P., Bill, J., Steeb, S. and Aldinger, F., X-ray and neutron small angle scattering with Si–C–N ceramics using isotopic substitution. *Solid State Ionics*, 1997, **101–103**, 1041–1047.
26. Ténégal, F., Flank, A. M. and Herlin, N., Short range atomic structure description of nanometric Si/C/N powders by X-ray absorption spectroscopy. *Phys. Rev. B.*, 1996, **54**(17), 12029–12035.
27. See for example: Kaplan, S., Jansen, F. and Machonkin, M., Characterisation of amorphous carbon-hydrogen films by solid-state nuclear magnetic resonance. *Appl. Phys. Lett.*, 1985, **47**, 750–753.
28. Seifert, H. J., Peng, J. and Aldinger, F., Phase equilibria and thermal analysis of Si–C–N ceramics. *J. Alloys Comp.*, 2001, **320**, 251–261.